Annu. Rev. Fluid Mech. 2004. 36:121–47
doi: 10.1146/annurev.fluid.36.050802.121918

BIOFLUID MECHANICS IN FLEXIBLE TUBES

James B. Grotberg[1] and Oliver E. Jensen[2]
[1]*Biomedical Engineering Department, University of Michigan, Ann Arbor, Michigan 48109-2099; email: grotberg@umich.edu*
[2]*School of Mathematical Sciences, University of Nottingham, University Park, Nottingham NG7 2RD, United Kingdom; email: Oliver.Jensen@nottingham.ac.uk*

Key Words fluid-structure interaction, free-surface flows, collapsible tubes, physiological fluid dynamics, surface tension, Starling Resistor, airway closure, airway reopening

■ **Abstract** Almost all vessels carrying fluids within the body are flexible, and interactions between an internal flow and wall deformation often underlie a vessel's biological function or dysfunction. Such interactions can involve a rich range of fluid-mechanical phenomena, including nonlinear pressure-drop/flow-rate relations, self-excited oscillations of single-phase flow at high Reynolds number and capillary-elastic instabilities of two-phase flow at low Reynolds number. We review recent advances in understanding the fundamental mechanics of flexible-tube flows, and discuss physiological applications spanning the cardiovascular system (involving wave propagation and flow-induced instabilities of blood vessels), the respiratory system (involving phonation, the closure and reopening of liquid-lined airways, and Marangoni flows on flexible surfaces), and elsewhere in the body (involving active peristaltic transport driven by fluid-structure/muscle interactions).

1. INTRODUCTION

When a flow is driven through a deformable channel or tube, interactions between fluid-mechanical and elastic forces can lead to a variety of biologically significant phenomena, including nonlinear pressure-drop/flow-rate relations, wave propagation, and the generation of instabilities. Understanding the physical origin and nature of these phenomena remains a significant experimental, analytical, and computational challenge, involving unsteady flows at low or high Reynolds numbers, large-amplitude fluid-structure interactions, free-surface flows, and intrinsically 2D or 3D motion. Whereas frequently the internal flow involves a single fluid phase (albeit often of a complex biological fluid such as blood), in many instances the presence of two or more distinct flowing phases is of primary importance (as is the case for air-liquid flows in peripheral lung airways, for example). We divide this review accordingly: Section 2 treats single-phase flows in collapsible tubes, Section 3 covers recent applications of such flows to a wide range of physiological

systems, and Section 4 surveys two-phase flows in flexible tubes and channels (with largely respiratory applications).

2. SINGLE-PHASE FLOW IN COLLAPSIBLE TUBES AND CHANNELS: THEORY AND EXPERIMENT

The biological applications that have motivated much of the work on flows in collapsible tubes and channels, and some of the relevant modeling, are well documented elsewhere (Carpenter & Pedley 2003, Grotberg 1994, Grotberg 2001, Kamm 1987, Kamm & Pedley 1989, Ku 1997, Pedley & Luo 1998, Shapiro 1977a, Shapiro 1977b). Our survey here is necessarily selective, but aims to complement these earlier reviews. It is helpful to focus our discussion of modeling developments of single-phase flows around a widely used experimental system (the Starling Resistor). First, however, we quickly review some flows in the body where vessel flexibility is significant.

2.1. Primary Biological Applications

The cardiovascular system provides abundant examples of sites where flow-structure interactions are of major biological importance (Shapiro 1977a). Most obviously, pulse propagation in arteries is fundamental for transporting blood from the heart to tissues and organs throughout the body. Under normal conditions arteries are under sufficiently large transmural (internal minus external) pressure to remain distended and stiff, so that wall strains are typically small. Important exceptions are the coronary arteries, embedded in the muscular wall of the heart, which can be significantly constricted as the heart contracts (Guiot et al. 1990), and the brachial artery, which is compressed by a cuff inflated around the upper arm during blood-pressure measurement, in which case flow-induced instabilities generate clinically useful "Korotkoff sounds" (Bertram et al. 1989, Ur & Gordon 1970). Veins operate under much lower transmural pressures than arteries so that hydrostatic pressure variations (in systemic veins above the heart but outside the skull, or in the pulmonary circulation) can be sufficient to induce collapse (i.e., a significant reduction in cross-sectional area, but without complete occlusion), which can limit the flow of blood returning to the heart or passing through major organs such as the lungs. Venous collapse is important during exercise, when muscular compression of leg veins is used to pump blood against gravity up to the heart, and in therapeutic compression of leg veins for the treatment of deep-vein thrombosis (Dai et al. 1999). Flow-induced instabilities in the venous system can lead to palpable thrills or audible murmurs, for example in the collapsed external jugular vein in the neck of an upright subject (Danahy & Ronan 1974).

The airways throughout the respiratory system are deformable to a degree, and flow-structure interactions underlie a number of important pulmonary conditions. Expiratory flow limitation is of particular significance: An increase in effort (i.e., driving pressure drop) during forced expiration, at a given lung volume,

can lead to no increase, and possibly a decrease, in the flux of expired air, essentially because the driving upstream (alveolar) pressure leads to compression of conducting airways. This maneuver is often accompanied by wheezing, arising from a flow-induced instability of deformable airway walls. Inspiration can lead to flow-induced upper-airway obstruction (contributing to sleep apnea) and instabilities that generate snoring noises. More controlled noise generation arises in the larynx, where flow-induced oscillations of the vocal chords generate speech. Elsewhere in the body, deformability is significant in peristaltic transport, for example through the intestines and the urogenital tract.

2.2. Experiments: The Starling Resistor

The classical bench-top experiment used to investigate such applications is the Starling Resistor (Knowlton & Starling 1912). A segment of elastic tubing is mounted between two rigid tubes and is enclosed in a chamber maintained at a fixed pressure p_e (Figure 1). A flux Q of fluid is driven through the device by an imposed pressure drop $p_u - p_d$, typically at Reynolds numbers Re based on tube diameter in the range 10^2–10^4. The pressures at the upstream and downstream ends of the collapsible segment (p_1 and p_2, respectively) are measured and may be controlled by valves providing additional upstream and downstream flow resistance in the rigid parts of the apparatus. In the absence of any flow ($p_u = p_d$), an increase in p_e generates a compressive stress in the tube wall causing it to buckle from a circular to an elliptic cross-section (except, of course, near its ends, where it is attached to the rigid tubes). Buckling to a shape with more than two lobes may arise in short, tethered, or inhomogeneous tubes. Once buckled, the tube becomes highly compliant so that small additional increases in p_e lead to a substantial reduction in cross-sectional area α. Further compression leads to contact of the opposite tube walls, first at a point, and then along a line (Figure 2, left); once in opposite-wall contact, the tube's compliance falls because strong bending forces in the tube wall at the bulbous end of each lobe provide an increasing resistance to area reductions. The "tube law," the relation between transmural pressure $p - p_e$ (where p is the internal pressure) and α, for a long thin-walled tube can be approximated by thin-shell theory for an axially uniform elastic ring (Flaherty

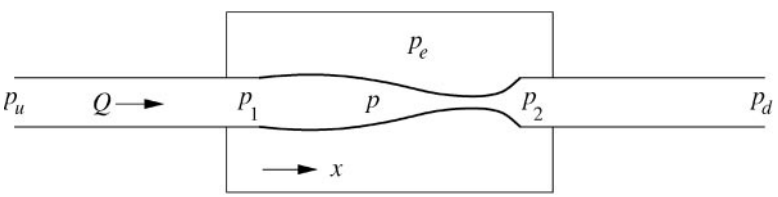

Figure 1 A Starling Resistor: a collapsible tube is mounted between two rigid tubes and is enclosed in a chamber held at pressure p_e. Flow with volume flux Q is driven by the imposed pressure drop $p_u - p_d$.

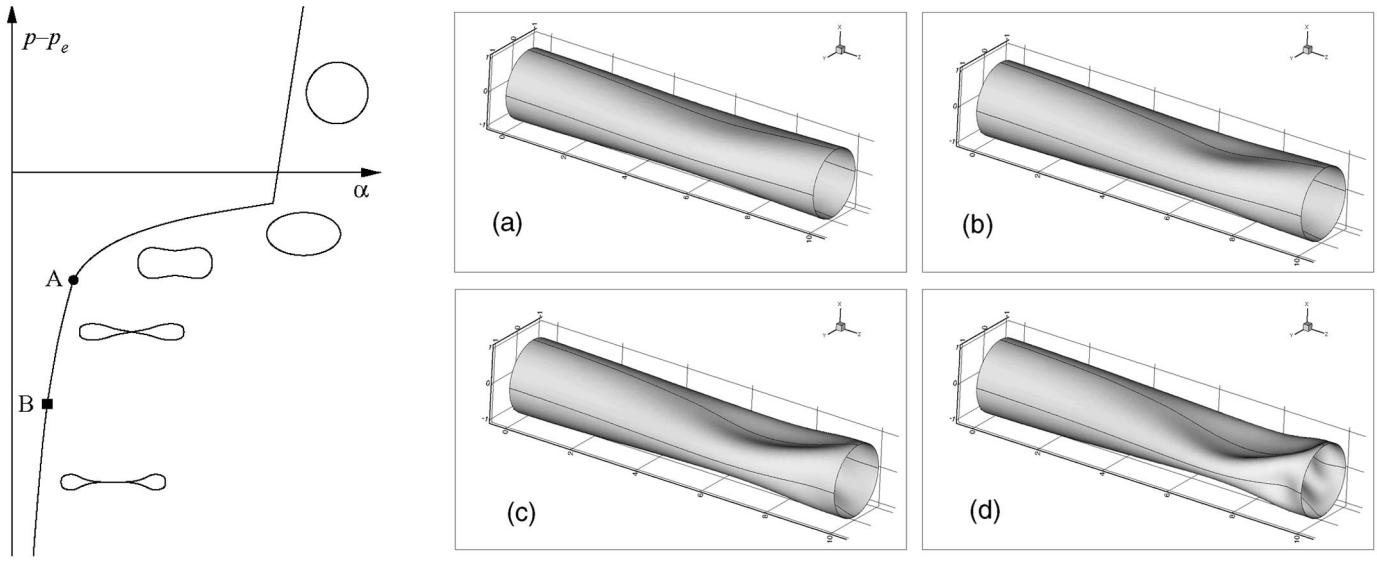

Figure 2 *Left*: a schematic tube law, relating transmural pressure $p - p_e$ to cross-sectional area α, with sketches of typical cross-sections. The tube's walls are in point contact between A and B, and in line contact beneath B. *Right*: computations using geometrically nonlinear shell theory, demonstrating 3D buckling and collapse of a tube held open at each end, supporting an internal flow; external compression increases from panel (a) to panel (d) (from Heil 1997).

et al. 1972); this predicts that the primary buckling instability is supercritical and yields the self-similar relation $p - p_e \sim \alpha^{-3/2}$ for line contact (Figure 2, left). More sophisticated models, using for example 3D geometrically nonlinear shell theory (Figure 2, right), capture the effects of mounting onto rigid tubes, axial prestretch and, potentially, subcritical buckling instabilities (Heil & Pedley 1996).

If a flow is driven through a Starling Resistor (with $p_u > p_d$ in Figure 1), then as p_e is increased a constriction typically forms first toward the collapsible tube's downstream end (where internal pressure is lowest) (Figure 2, right). Various experimental protocols can then be followed, such as increasing the pressure drop along the tube $p_1 - p_2$ while keeping the upstream transmural pressure $p_1 - p_e$ fixed (which leads to "flow limitation," i.e., a limit in the maximum possible Q), or increasing Q while keeping $p_2 - p_e$ fixed (which leads to "pressure drop limitation," i.e., a restriction on the largest value of $p_1 - p_2$). Of all who have examined this system, Bertram and coworkers (e.g., Bertram 1986; Bertram et al. 1990, 1991) characterized it in greatest detail. In particular, using water in thin-walled tubes, they mapped out regions in parameter space in which the system exhibits spontaneous and often vigorous oscillations. These arise in distinct frequency bands (from a few up to hundreds of hertz), are strongly dependent on the properties of the rigid parts of the system, and exhibit hysteresis between both steady and dynamic states, accompanied by strong evidence of nonlinear phenomena such as mode interactions and probably (but not definitively) chaotic behavior. This is a particularly rich dynamical system because of the complexity of the internal flow, which can be turbulent under typical operating conditions. The internal structure of steady 3D flow beyond the 2-lobed "throat" of a collapsed tube was recently visualized (Bertram & Godbole 1997), revealing axially decaying twin jets with a region of reversed flow in between. The difficulty of measuring and visualizing flow inside an oscillating elastic tube is a formidable task, although laser-Doppler velocimetry results are now becoming available (e.g., Bertram et al. 2001). When air, not water, is used for the internal flow (to mimic lung airways), making the inertia of the tube wall comparable to that of the fluid, noisy high-frequency flutter instabilities are readily generated, typically when the device exhibits flow limitation (Gavriely et al. 1989). In the following sections, it is convenient to distinguish between what are generally called self-excited oscillations (relatively low-frequency oscillations for which membrane inertia is not a critical factor) and flutter (high-frequency oscillations for which membrane inertia is generally significant), although this distinction is sometimes blurred.

2.3. Theoretical Models

Theoretical models of incompressible flow through the Starling Resistor, or through an analogous 2D system introduced by Pedley (1992) (a finite-length channel, in which a segment of one wall is replaced by a membrane under longitudinal tension, see Figure 3), developed from lumped-parameter models to spatially distributed 1D, 2D, or 3D models. Much of this modeling effort was recorded in detail

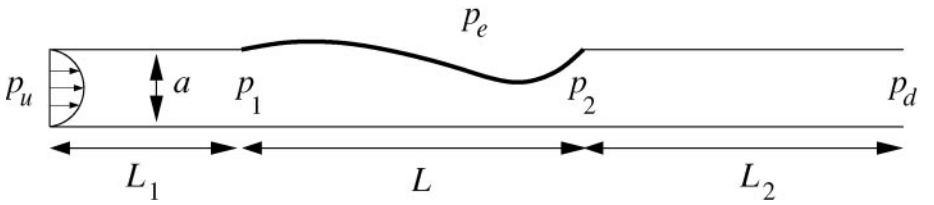

Figure 3 A 2D channel of length $L_1 + L + L_2$ and undisturbed width a, containing a membrane under tension; flow is driven through the channel either with imposed flux or imposed pressure drop $p_u - p_d$.

elsewhere (Heil & Jensen 2003, Pedley & Luo 1998, Shapiro 1977b), so we discuss only some of the more significant and recent contributions.

2.3.1. ONE-DIMENSIONAL MODELS Although being ad hoc to a degree, 1D models have proven a powerful tool in understanding a wide range of collapsible-tube flows. These models involve partial differential equations (PDEs) describing mass and momentum conservation, coupled through a local pressure/area relation, typically taking the form

$$\alpha_t + (u\alpha)_x = 0 \tag{1a}$$

$$\rho(u_t + uu_x) = -p_x - F \tag{1b}$$

$$p - p_e = P(\alpha) - T\alpha_{xx}. \tag{1c}$$

Here x measures axial distance along the tube, t time, $\alpha(x, t)$ the tube's cross-sectional area, $u(x, t)$ and $p(x, t)$ the cross-sectionally averaged axial velocity and pressure, ρ the constant fluid density, and subscripts x and t derivatives. The term $F \geq 0$ represents viscous dissipation, either distributed frictional losses (e.g., $F = F(u, \alpha)$) or quasi-steady losses arising in a region of separated flow [e.g., $F = (\chi - 1)\rho u u_x$, in which $\chi = 1$ where the flow is fully attached and $0 < \chi < 1$ where it is separated and $u_x < 0$ (Cancelli & Pedley 1985)]. The nonlinear tube law $P(\alpha)$ in Equation 1c characterizes the highly variable compliance of the tube as it changes from being distended ($p > p_e$) to buckled or highly compressed ($p < p_e$); a simple algebraic approximation to the graph shown in Figure 2 (e.g., Elad et al. 1987) is effective for many applications. The tube law in Equation 1c is here accompanied by a term $T\alpha_{xx}$, approximating the effects of constant longitudinal tension T, where α_{xx} approximates the longitudinal curvature of the tube wall. Further terms representing bending stiffness, wall damping, and wall inertia can be included in Equation 1c. These terms can have an important effect in stability analysis of flow-structure interactions because in their absence such problems can exhibit singular behavior.

The PDEs in Equation 1a–c with $T = 0$ are closely related to those describing compressible-gas and shallow-water flows, and so many features of these widely

studied systems carry over to collapsible-tube flow, including wave propagation [small-amplitude pressure waves propagate along the tube with speed $u \pm c$, where $c^2 = \alpha P'(\alpha)/\rho$], choking [for steady subcritical flows (with $0 < u < c$) in the presence of friction, $\alpha \to 0$ at sufficiently large, finite x], steady sub- to supercritical flow transitions (forced by suitably chosen variations in p_e, or material properties), and abrupt super- to subcritical transitions via an elastic jump (the analogue of a hydraulic jump in shallow-water flow). Propagating elastic jumps arise at the leading edge of roll waves, for example, which Brook et al. (1999) predicted to form spontaneously in long inclined collapsible tubes using numerical shock-capturing techniques.

Supercritical flow provides a possible mechanism of flow limitation: If $u > c$ and $T = 0$, waves cannot in principle propagate upstream into a region of supercritical flow, and a reduction in downstream pressure cannot lead to an increase in flow rate. Though recent experiments show that flow limitation is a necessary but not sufficient condition for the onset of self-excited oscillations or flutter (Bertram & Castles 1999, Gavriely et al. 1989), 2D computational studies that take full account of effects such as viscous dissipation and longitudinal tension (see below) suggest there is no direct link between the onset of supercritical flow and the growth of these instabilities (Luo & Pedley 1998, 2000). However, recent 2D simulations of steady flow in an axisymmetric elastic tube (Shim & Kamm 2002) support the wave-speed concept of flow limitation predicted by 1D models, even when membrane tension and bending stiffness allow short waves to propagate upstream through a region of supercritical flow.

An important reason for including the tension term in Equation 1c is to match the order of the PDEs to the four boundary conditions required to describe flow in the Starling Resistor: These fix the area at either end of the collapsible segment and relate the pressure to the local axial velocity, accounting for the viscous resistance and fluid inertia in the rigid tubes. Then, neglecting frictional effects, Equations 1a–c predict choking [$\alpha \to 0$ in finite time (Cancelli & Pedley 1985), a manifestation of so-called static divergence instability], but including dissipation, either through a distributed frictional term (Hayashi et al. 1998) or through Cancelli & Pedley's (1985) $F = (\chi - 1)\rho u u_x$ term, leads to a rich variety of self-excited oscillations (e.g., Cancelli & Pedley 1985, Hayashi et al. 1998, Jensen 1992, Matsuzaki et al. 1994). These oscillations arise in distinct frequency bands, as seen experimentally because they originate as normal modes of the system, each with a discrete number of wavelengths along the collapsible segment (Jensen 1990). Nonlinear mode interactions give rise to complex dynamical behavior (Jensen 1992) reminiscent of that seen experimentally.

While 1D models provide significant insights, they fail to provide reliable quantitative matches with experiment. Neither the representation of viscous dissipation for high-*Re* flow in Equation 1b, nor the modified tube law in Equation 1c, is derived rationally from a higher-order system, and both can exhibit significant qualitative deficiencies (particularly, for example, in describing energy losses associated with unsteady flow separation). Furthermore, a 1D framework cannot be

guaranteed to capture all possible modes of instability known to be present in systems involving flows over compliant surfaces, such as Tollmien-Schlichting (TS) waves or traveling-wave flutter (TWF) (Carpenter & Garrad 1985, 1986). Thus, in the 1980s and 1990s, attention turned to the development of rational 2D models. Two classes of model are important here: those describing small-amplitude instabilities in spatially uniform, unbounded elastic-walled channels, and those describing flow in a finite-length channel with a section of one wall replaced by a segment of membrane under longitudinal tension (Figure 3).

2.3.2. TWO-DIMENSIONAL MODELS OF UNBOUNDED FLOWS Stability analysis of small-amplitude disturbances to unbounded flow in a spatially uniform compliant channel, based on the Orr-Sommerfeld equation and accounting for wall inertia, damping, bending stiffness, tension and a spring-backing, has revealed multiple modes of instability. [These have been investigated in detail in the context of open flows over compliant surfaces, normally with the motivation of delaying transition to turbulence. We restrict attention here to channel flows; for reviews of relevant early work see LaRose & Grotberg (1997) and Davies & Carpenter (1997a).] The three modes most commonly encountered are conveniently described using the well-known Benjamin-Landahl energy classification: TS waves (modified by wall flexibility) are Class A (stabilized when energy is transferred irreversibly from the flow to the wall, thus destabilized by wall damping–for these so-called "negative energy waves" damping increases the wave energy while reducing the overall energy in the system); TWF is Class B (destabilized when energy is transferred from the flow to the wall, thus stabilized by wall damping); and static divergence is Class A or C (the latter being relatively indifferent to the direction of energy transfer). TS waves and TWF are convective instabilities, whereas static divergence can give rise to low (or zero) frequency oscillations that are absolutely unstable. TWF relies on pressure and displacement at the wall being out of phase with one another so that work can be done on the wall. This phase shift can arise through an inviscid mechanism confined to critical layers (Davies & Carpenter 1997a, Huang 1998, Miles 1957). Additional modes of instability have also been identified: Davies & Carpenter (1997a) showed how an interaction between TS and TWF modes can be strongly unstable; LaRose & Grotberg (1997) identified an apparently distinct long-wave instability of developing flow in a compliant channel; and Walsh (1995) identified a long-wave flutter mode that arises when coupling between transverse and longitudinal wall strain is significant. Kumaran and coworkers also highlighted the limitations of representing the compliant wall as a membrane or plate that moves only in the transverse direction. In an extensive series of papers, they identified novel viscous and inviscid instabilities of flows over gel-like viscoelastic surfaces in which axial and transverse motions of the wall are coupled. This coupling allows energy to be transferred from the mean shear flow to fluctuations through work done at the wall, even in the limit of zero *Re*. This yields, for example, a viscous mode of instability not present in rigid systems. This has a counterpart at high *Re*, operating through a similar energy-transfer mechanism,

for which viscous stresses are confined to a wall layer of thickness $Re^{-1/3}$ relative to the channel width. A further new inviscid mode, distinct from TS instability, grows via energy transfer arising from Reynolds stresses within a critical layer, also of thickness $Re^{-1/3}$. Shankar & Kumaran (1999) and Kumaran (2000, 2003) reviewed this family of instabilities in more detail.

2.3.3. TWO-DIMENSIONAL MODELS OF BOUNDED FLOWS Studies of small-amplitude disturbances in spatially unbounded channel flows highlight a wide range of potential instabilities, but provide only a limited guide to behavior in spatially inhomogeneous or bounded systems. Because a key feature of the Starling Resistor is its finite spatial extent, an alternative approach has been to consider the asymmetric 2D system illustrated in Figure 3. The flow here is driven by a fixed pressure drop or fixed upstream or downstream flux, and contains a finite-length membrane that can in principle undergo large-amplitude deformations.

Many workers have considered this problem when deflections of the compliant segment are small relative to the channel width. Replacing the membrane by a compliant panel, Davies & Carpenter (1997b) used a novel computational formulation of the linearized Navier-Stokes equations to show how energy can be transferred between TS and TWF modes at the panel's boundaries. Treating the flexible segment as a membrane and assuming $Re \gg 1$, Guneratne (1999) used interactive boundary-layer theory to describe steady flows: when $p_e = 0$ and the membrane tension T is reduced from an initially large value, the system exhibits an increasing number of static eigenmodes arising via static divergence instability; nonzero p_e breaks the symmetry of the solution structure so that as T falls one passes through regions of parameter space exhibiting single, multiple, or no steady solutions. Huang (2001) assumed that the membrane has inertia, damping, and relatively low tension, and that p_e is chosen to ensure the existence of a uniform steady solution. Analyzing the linearized Navier-Stokes equations numerically, he showed how the system exhibits both static divergence (at sufficiently low tension) and flutter (dependent on membrane inertia), with both sensitive to the choice of upstream and downstream boundary conditions.

The richness of the behavior revealed by these simplified studies is reflected by Navier-Stokes simulations of steady laminar flows in the system shown in Figure 3, at $Re \equiv \rho Ua/\mu$ of up to a few hundred, where a is the channel width, U the input flow speed, and μ the dynamic viscosity. These finite-element schemes, in which the fluid and solid solvers are fully coupled (Luo & Pedley 1995, 1996; Rast 1994; Shim & Kamm 2002), predict steady membrane configurations similar to those of 1D models, flow separation downstream of the asymmetric indentation, and sometimes a long-wavelength nonlinear standing wave in the flow beyond the constriction, in which the inviscid core flow sweeps abruptly from wall to wall, with regions of wall-bound separated flow on both walls of the channel. Luo & Pedley (1996) showed how these steady flows can become unstable to self-excited oscillations if Re is sufficiently high or the membrane tension sufficiently low. In their simulations, membrane oscillations generate (or are possibly generated by)

downstream propagating waves in the inviscid coreflow beyond the constriction. These are "vorticity waves," large-amplitude inviscidly generated TS waves described previously via experiments, simulations, and analysis of flow through a channel with a deformable segment of wall that oscillates in a prescribed manner (e.g., Pedley & Stephanoff 1985, Ralph & Pedley 1988) under conditions of $Re \gg 1$ and frequency $\omega \ll \mu/\rho a^2$. Although this striking activity occurs downstream of the collapsed segment, Luo & Pedley (1996) found that the dominant dissipation occurs, surprisingly, in viscous boundary layers on the channel walls upstream of the constriction. Subsequently, Luo & Pedley (1998) showed how introducing inertia in the membrane allows an additional high-frequency flutter mode to grow. They also showed how the primary instability is sensitive to the choice of boundary conditions, being more stable when the upstream flux is prescribed rather than the pressure drop, for example (Luo & Pedley 2000).

Exploiting the simplification of large membrane tension so that the system shown in Figure 3 has a unique steady solution in which the membrane is almost flat, Jensen & Heil (2003) used a combination of asymptotic and computational methods to characterize in detail a mechanism of self-excited oscillation. When viscous effects are weak, the initially uniform membrane supports a family of high-frequency inviscid normal modes, in which transverse membrane deflections generate predominantly axial oscillations of the fluid in the entire channel. A scaling analysis shows that their frequency ω scales like $\omega^2 \sim aT/\rho L^4$, where L ($\gg a$) is the membrane length (which is representative of the lengths L_1 and L_2 of the upstream and downstream rigid segments, see Figure 3). If $L_1 < L_2$, the greater downstream fluid inertia suppresses fluctuations so that the modes have greater amplitude at the upstream end of the collapsible segment. An oscillating normal mode can then extract energy from an imposed pressure-driven flow (with mean speed U, for example) because kinetic energy fluxes into the upstream end of the collapsible segment of the channel (where oscillatory amplitudes are larger) exceed those out of the downstream end. For small-amplitude, neutrally stable oscillations, a balance between the energy extracted from the mean flow with that dissipated in viscous boundary layers (Stokes layers) along the channel walls, of thickness $(\mu/\rho\omega)^{1/2}(\ll a)$, provides an estimate of the critical Reynolds number for the onset of oscillations, namely $Re = O((\rho aT/\mu^2)^{1/4})$. A formal asymptotic analysis yields the prefactor in this relationship, which has a strong dependence on L_1 and L_2 (going to infinity as $L_2 \to L_1+$, for example). Jensen & Heil (2003) then used Navier-Stokes simulations to verify the accuracy of these asymptotic predictions and showed that the same mechanism persists at large amplitudes; no significant vorticity waves are generated in this case (because $\omega \gg \mu/\rho a^2$), although the flow exhibits a rich variety of secondary instabilities, located primarily toward the upstream end of the collapsible segment. This class of self-excited oscillation is a global mode of the entire system, not relying on intrinsic local hydrodynamic (TS or flutter) modes, but requiring dissipation (in this case Stokes layers) to avoid static divergence. It remains to be seen whether this or another mechanism underlies the low-frequency self-excited oscillations described by Luo & Pedley (1996).

2.3.4. THREE-DIMENSIONAL MODELS To describe the 3D flow-structure interactions arising in the Starling Resistor, Heil and coworkers used finite-element methods to couple geometrically nonlinear Kirchoff-Love shell theory (allowing both large deformations and small strains) to an internal 3D Navier-Stokes flow. Restricting attention initially to Stokes flows, or to lubrication theory (which works remarkably well in this problem at low *Re*), they showed how nonaxisymmetric buckling of the tube (e.g., Figure 2, right) contributes to nonlinear pressure-flow relations that can exhibit flow limitation through purely viscous mechanisms (Heil 1997, Heil & Pedley 1996). For short tubes under compression, the buckling instability may be subcritical, leading to hysteresis in the pressure-flow relation, so that an initially open tube "snaps through" to a collapsed state that under certain conditions may have the tube's opposite walls in contact. Heil's (1997) Stokes-flow simulations (Figure 2, right) show excellent agreement with experiment. These computations were recently extended to describe steady 3D flows in nonuniformly buckled tubes at *Re* of a few hundred (Hazel & Heil 2003). These studies reveal twin jets emerging from the 2-lobed throat, with reversed flow between them; the jets broaden and merge further downstream, consistent with Bertram & Godbole's (1997) observations. Whereas these computations assume the flow has a fourfold symmetry, observations on a collapsible-tube system (Kounanis & Mathioulakis 1999) show a jet emerging from a constriction that remains attached to one wall (via the Coanda effect), with flow separation occurring on the other, a flow with only twofold symmetry. It is an open question whether symmetry breaking underlies a further potential mechanism of instability in this system.

3. SINGLE-PHASE FLEXIBLE-TUBE FLOWS: BIOLOGICAL APPLICATIONS

The Starling Resistor has attracted significant interest from experimentalists and theoreticians. It is simple to operate, exhibits dramatic flow-structure interactions, and presents a wealth of modeling opportunities. However, it is only a model system and it is easy to be diverted from the physiological flows that provided its original motivation. We therefore return to some biological applications.

3.1. Flow Limitation

One-dimensional models for flow limitation in the lung during forced expiration are now well developed and have been described elsewhere (Grotberg 1994). A novel application of 1D modeling of flow limitation is the giraffe jugular vein (Pedley et al. 1996). Because measurements show that the internal pressure in the vein increases with height (rather than falling hydrostatically), it is inferred that the jugular vein is strongly collapsed, offering large viscous resistance. Simulations suggest the highly collapsed region terminates at its downstream end with an elastic jump, returning a subcritical flow to the heart. However, too high a flow rate moves

this jump toward the heart until steady flow is no longer possible, and instead the system exhibits irregular small-amplitude oscillations that effectively limit the flow (Brook & Pedley 2002). Flow limitation is also an important regulatory mechanism during postural changes. As a giraffe lifts its head from drinking, there is rapid emptying of the jugular vein, but its rapid collapse prevents excessive flow rates from developing.

3.2. Wave Propagation

Small-amplitude wave propagation in elastic tubes, described by linear or weakly nonlinear analysis, has an extensive literature that we do not attempt to survey here, noting only that Pedley (1980) provides an introduction to wave attenuation due to viscous losses, tapering, tethering, branching, and so on, and many others (e.g., Demiray 1996) have treated topics such as solitary wave formation. The maturity of theoretical developments means that recent interest has turned instead to specific applications, such as the effect on pulse-wave propagation of surgical interventions such as vascular stents and grafts. A mismatch in diameter or compliance between native and artificial material can induce wave reflections and flow disturbances that may promote disease processes in the arterial wall, mediated for example by altered wall shear-stress distributions (Salacinski et al. 2001). For example, Wang & Tarbell (1992, 1995) showed how the phase difference between pressure and flow rate in oscillatory flexible-tube flow, which is altered by wave reflections, influences the steady-streaming flows driven by nonlinear convective accelerations, lowering the wall shear-stress distribution and making it more oscillatory, thereby promoting atherogenic risk factors. Progress in measuring the degree of wave reflection in biological vessels has been achieved through the use of "wave intensity analysis" (Khir et al. 2001, Parker & Jones 1990), a time-domain method based on the method of characteristics in which the local wave-speed is determined from simultaneous velocity and pressure measurements, allowing forward and backward propagating waves to be identified.

The importance of flow patterns in the development of arterial disease has motivated many computational simulations of flows in large arteries, a subset of which have included the effects of compliant boundaries. For example, Perktold & Rappitsch (1995) coupled (iteratively) geometrically nonlinear shell theory to a Navier-Stokes solver in a model of the carotid artery bifurcation, and showed a modest quantitative decrease in wall shear-stress magnitude relative to the rigid-walled case; in other cases, distensibility was less significant than variations in arterial geometry, for example (Steinman & Ethier 1994). A key prediction of such calculations is the level of flow-induced arterial wall strain, for example in a bypass graft, which is an important factor in understanding the causes of graft failure (Leuprecht et al. 2002). Flow-structure interactions are possibly more significant in pathological conditions such as aortic dissection, in which blood enters the vessel wall through a tear in the intima or intramural hemorrhage, and then the tear propagates through the wall, possibly leading to rupture of the vessel (Tam et al. 1998).

A less familiar site of wave propagation is the spinal cord: This contains cerebrospinal fluid and occupies a rigid fluid-filled cavity (the subarachnoid space) running from the base of the skull down to the base of the spine. A cough or a sneeze creates waves that propagate along the cord that may steepen to form propagating elastic jumps. At a blockage, reflection of a shock would create localized pressure variations that (it is hypothesized) lead to the formation of longitudinal cavities in the spinal cord. A 1D inviscid model of this process, treating the spinal cord as a flexible tube, confined within a rigid fluid-filled coaxial cylinder, has been used to investigate this potential mechanism of the disease syringomyelia (Carpenter et al. 1999).

3.3. Self-Excited Oscillations

An important and potentially dangerous manifestation of self-excited oscillation arises in arterial stenoses (Ku 1997). High flow speeds through a narrow stenosis lead to low pressures, which can induce arterial collapse, flow limitation, and possible flow-induced instabilities. The resulting static and dynamic loading on the diseased arterial wall may be sufficiently vigorous or sustained to fracture the stenosis' plaque cap, causing fragments to be swept downstream, a possible precursor of heart attack or stroke. Ku (1997) reviewed early 1D models of this process, which show how supercritical flow downstream of the stenosis terminates in an elastic jump, a configuration leading to flow limitation. More realistic computational models have been developed subsequently, including those of Bathe & Kamm (1999) and Tang et al. (1999), both of which involve computational studies of axisymmetric interactions between a high-*Re* laminar flow and a nonlinearly elastic tube wall that incorporates a high-grade stenosis. Despite modest differences in models and methods (e.g., a fully coupled versus an iterative numerical scheme, unsteady versus quasi-steady flows, large versus small axial prestretch), they both provide estimates of damagingly high shear stresses exerted on endothelial cells and large cyclical compressive stresses in the downstream shoulder of the stenosis.

Self-excited oscillations are responsible for the generation of speech in the human larynx and bird-song in the avian syrinx. Flow through the larynx generates instabilities of the vocal chords, which excite acoustic modes in the upper airways. Theoretical models of phonation have a long history (to which full justice cannot be done here), going back to the influential lumped-parameter model of Ishizaka & Flanagan (1972), in which the glottal wall is characterized by two independent masses. Low Bernoulli pressures and elastic recoil pull the walls of the glottis together, leading to complete but transient airway occlusion; the continuing flow of air from the lungs causes pressure to build up sufficiently to reopen the glottis; this sequence then repeats at a frequency dictated by factors including wall inertia and viscoelasticity. Numerous modifications of this model have since been developed, for example capturing more accurately the mechanical properties of the oscillating glottis walls (Story & Titze 1995) or exploring the model's nonlinear dynamics (Steinecke & Herzel 1995). Representation of the internal fluid dynamics has also been refined substantially, from 1D distributed collapsible-tube models that enable

wall collision (Ikeda et al. 2001), to 2D Navier-Stokes simulations, either with prescribed wall motion (Zhao et al. 2002) or coupled to a lumped-parameter model of wall mechanics (de Vries et al. 2002). Acknowledging that the jet emerging from the glottis is in reality turbulent, Zhao et al.'s (2002) computations of compressible, laminar flow capture unsteady vortex shedding beyond the constriction, at a rate influenced by the frequency of glottis motion, and demonstrate that the glottis acts as a compact acoustic source, predominantly as a dipole (due to the presence of a mean flow) rather than a monopole (due to volume changes), at least at low frequencies. For a recent survey of models for other respiratory noises (such as wheezing or snoring), see Grotberg (2001).

3.4. Active Motion

Many vessels conveying fluids through the body transport their load using peristalsis, active muscular compressions of the vessel wall; examples include the esophagus, gut, ureter, and uterus (Eytan & Elad 1999). Peristaltic flows driven by prescribed wall motions have been investigated intensively over many years. Recent models have addressed the significance of unsteadiness arising from end effects in finite-length channels (Li & Brasseur 1993), steady-streaming flows and their mixing properties (Selverov & Stone 2001, Yi et al. 2002) (with applications to microfluidic devices with flexible walls), and the physiological and mechanical advantages arising from longitudinal shortening of the vessel wall, such as occurs during muscular contractions in the esophagus (Pal & Brasseur 2002). Fewer investigators have considered how the muscular wall responds to flow-induced forces, treating it as a free boundary. Griffiths (1989) modeled the ureter as a finite-length collapsible tube subject to a prescribed, moving external pressure distribution, finding an upper limit on the frequency of propagating waves for which peristaltic transport is effective. Allowing the wall to respond to the forces placed upon it is important because, in the presence of a mean pressure gradient, a moving external pressure distribution can generate traveling waves that propagate away from the disturbance, as Kriegsmann et al. (1998) showed for the closely related case of a thin viscous fluid layer subject to external pressure forcing. Going a step further, it is necessary to integrate muscle, solid, and fluid mechanics. For example, Carew & Pedley (1997) developed a model of flow in the ureter using a constitutive relation for the muscular wall that incorporates passive viscoelasticity with active force generation dependent on electrical stimulation, local muscle stretch, and rate of stretch. Their model predicts the phase lag between stimulation and constriction arising from flow-structure muscle interaction, for example.

4. MULTIPHASE FLOWS IN FLEXIBLE TUBES

The cardiovascular system has been a dominant source of applications of studies of flows in flexible tubes. The airways of the lung provide a further source of important problems where multiphase fluid mechanics has important biological

applications, involving flexible tubes with a liquid lining or a liquid occlusion. Below we review major recent developments for which wall flexibility is a critical factor. First, we consider how surface tension, elastic forces, and airflow together control the configuration of a deformable airway and its internal liquid lining. The primary aim is to determine the conditions leading to airway closure, whereby the liquid lining forms a plug occluding (and collapsing) the airway and inhibiting gas exchange. Second, we discuss mechanisms by which an initially occluded airway may be reopened by inflating the airway with an advancing air bubble, or by displacing a preexisting liquid plug. Finally, we examine liquid-lining flows driven by interactions between in-plane stretching of the airway wall and Marangoni forces due to the presence of surfactants.

4.1. The Capillary-Elastic Instability

4.1.1. AXISYMMETRIC FLOW AND DEFORMATION Motivated by airway closure dynamics in the lung, Halpern & Grotberg (1992) analyzed the stability of a liquid-lined, flexible tube under longitudinal tension. The system was assumed axisymmetric and the external pressure was held constant. Using lubrication theory and a modified form of the normal-stress boundary condition (Gauglitz & Radke 1988) to derive evolution equations that captured both the thin-film dynamics and quasi-static capillary surfaces, they showed that there is a critical film-thickness to tube-radius ratio, ε_c, above which disturbances grow via the Rayleigh instability to form liquid bridges. ε_c is strongly dependent on fluid and wall properties, decreasing with increasing surface tension or wall compliance. The important parameter reflecting the relative strengths of the mean surface tension σ_m, which is destabilizing, and wall elasticity, which is stabilizing, is $\Gamma = \sigma_m(1 - \gamma^2)/Eh_0$, where γ is the Poisson ratio of the tube material, E is its Young's modulus and h_0 is the tube wall thickness. For example, wall compliance in physiologic ranges of Γ, say $\Gamma \sim 0.1$, can reduce ε_c from a rigid-tube value of $\sim$0.17 to a flexible-tube value of 0.12 using a disturbance wavelength equal to the airway length. Airway closure occurs more rapidly with increasing unperturbed film thickness, surface tension, wall flexibility, and decreasing wall damping. Halpern & Grotberg (1993) subsequently showed that surfactant increases ε_c by as much as 60% for physiological conditions, and that the closure time for a surfactant-rich interface can be approximately five times greater than the surfactant-free system. Surfactant stabilizes the system both by reducing the overall surface tension and by introducing Marangoni stresses that slow the fluid flow feeding the growing disturbance. Otis et al. (1993) modeled a liquid-lined, rigid tube whose radius decreases with time at a prescribed rate to mimic exhalation. Their numerical results show that surfactant is effective in retarding or eliminating liquid bridging through the reduction of the mean surface tension and the action of surface tension gradients. The former effect is also critical in minimizing the magnitude of the negative pressure in the liquid layer and thus presumably in reducing the tendency for the airway to collapse along its length.

4.1.2. NONAXISYMMETRIC FLOW AND DEFORMATION Just as a flexible tube buckles under external compression (Figure 2), an airway wall under compression will likely buckle to nonaxisymmetric configurations with circumferential modes with wavenumber $n \geq 2$. The liquid lining of an airway then will likely form pools in the circumferential folds of the wall. The 2D model of Hill et al. (1997) investigated this situation, treating the airway as a thin-walled, elastic tube subject to a prescribed external pressure. The airway's configuration is determined by bending stresses in the wall and a compressive load arising in part from surface tension associated with liquid that partially fills the folds. Taking $n = 16$ (typical of values seen experimentally), they found that if the liquid volume is small (<2% of luminal volume), the air-liquid interface coincides with the fold-region's wall shape and surface tension does not significantly affect the relationship between cross-sectional area α and transmural pressure P. However, for fluid volumes >2%, surface tension contributes to airway compression and destabilizes the system. The shape of the static $\alpha(P)$ curve reveals two stable regions ($d\alpha/dP > 0$) connected by an unstable region ($d\alpha/dP < 0$). Snap-through from a stable, axisymmetric shape to a stable, partially collapsed state may therefore occur. The tube lumen always has an air core in this model, unlike that of Heil (1999a), who computed the 3D configuration of an otherwise dry tube that is occluded by a localized liquid plug with a finite contact angle. The static force balance, including external compression, for the $n = 2$ mode also predicts an $\alpha(P)$ curve with two stable limbs connected by an unstable solution. A stable axisymmetric shape can snap down to stable collapse with wall-wall contact over part of the cross-section. Larger surface tension permits an $n = 3$ mode to arise whose more complicated $\alpha(P)$ curve has stable, partially collapsed states without opposite-wall contact. In an extended treatment (Heil 1999b), this model also shows that the minimal volume of the liquid bridge can be much smaller than that required for closure in a rigid tube [experiments using rigid tubes predict critical volumes of 5.47 R^3 (Everett & Haynes 1972) and 5.6 R^3 (Kamm & Schroter 1989), where R is the tube radius]. This is expected because the walls are much closer together in a buckled tube, requiring less liquid to fill the gap. It was not clear from Heil's results whether or not the system could start from an axisymmetric state and buckle to a nonaxisymmetric shape resulting in closure, if the liquid volume were smaller than that required for axisymmetric closure. This question was addressed by Heil & White (2002), this time in 2D and with fluid flow, where the tube became occluded even if the volume of fluid in the liquid lining was much smaller than that required to cause occlusion in the axisymmetric state. Using a much simpler wall model, based on Euler-Bernoulli beam theory, a 2D quasi-static analysis in Rosenzweig & Jensen (2002) reached qualitatively similar conclusions, including the reduction in critical liquid volume. For example, their dimensionless ratio relating surface tension to wall elasticity is equivalent to Γ/δ^2, where $\delta = h_0/R$. Assuming zero external pressure, when $\Gamma/\delta^2 = 4$, their model predicts that closure can occur for an initial film thickness of 0.066 R in a circular tube.

Capillary-elastic instabilities are important in microscale biological phenomena where there may be more than one liquid layer. Pozrikidis (2000) treats an

annular system of two concentric liquid layers bounded externally and internally by rigid tubes, where the boundary between the liquids can have elastic properties in addition to surface tension. This is a model of lipid bilayers found in cell membranes and tubules. The surface tension is responsible for the Rayleigh capillary instability, but the elastic tensions resist the deformation and slow down or even prevent the growth of small perturbations.

4.1.3. STABILIZATION BY OSCILLATORY FORCING Collapse of an airway with liquid plugging eliminates gas exchange through the airway until it is reopened. Thus, there may be reasons to prevent this instability at the outset. Halpern & Grotberg (2003) investigated the effects of an oscillatory flow imposed on the core fluid of a liquid-lined, rigid tube; such a flow could mimic breathing, for example. The oscillatory core flow exerts tangential and normal stresses on the air-liquid interface that can prevent closure by nonlinear saturation of the capillary instability. The stabilization mechanism is similar to that of a reversing butter knife, where the core shear wipes the growing liquid bulge back onto the tube wall during the main tidal volume stroke, but allows it to grow back as the stroke and shear turn around. To be successful, the leading film thickness ahead of the bulge must be smaller than the trailing film thickness behind it, a requirement necessitating that the bulge be swept along at large enough speeds. When this process is tuned correctly, the two phases balance and there is no net growth of the liquid bulge over one cycle.

4.2. The Motion of Long Bubbles in Flexible Tubes and Channels

4.2.1. EXPERIMENTS The propagation of an air finger into a liquid-filled, flexible tube arises in models of airway reopening, a process occurring during mechanical ventilation of diseased or injured lungs or during the initial opening of airways with a newborn's first breath. This important problem was initially examined by Gaver et al. (1990), in which airflow was forced into a one end of a long, thin-walled, polyethylene tube that was otherwise liquid-filled and flattened to a uniform thickness. They measured the relationship between the velocity, U, of the opening meniscus and the bubble pressure, P_b, while using tubes of different radii, R, and liquids with different viscosity, μ, and surface tension, σ. They found their data fit well to the dimensionless equation $P_b R/\sigma = 8.3 + 7.7Ca^{0.82}$, where the capillary number $Ca = \mu U/\sigma < 0.5$. When $Ca > 0.5$, viscous forces added appreciably to the overall opening pressures. As the formula indicates, steady reopening requires P_b to be in excess of a yield pressure, $P_y \sim 8.3\ \sigma/R$, a value consistent with physiologic experiments (Naureckas et al. 1994). A value of $P_y \sim 1.85\ \sigma/R$ in later 2D experiments of flexible channel opening (Perun & Gaver 1995a) indicated the importance of geometrical effects. Experiments conducted with prescribed bubble volume flux rather than prescribed pressure revealed transient overshoot in P_b during the initiation of bubble motion, and regimes of unsteady motion (Perun & Gaver 1995a, Perun & Gaver 1995b), features that may be significant

in clinical ventilation strategies. Issues similar to those arising in lung airways are also important in the Eustachian tube, which connects the middle ear with the nasal cavity. Ghadiali et al. (2002) introduced surfactants into the middle ear of monkeys to reduce surface tension of the liquid-lined (or partially filled) Eustachian tube. Their results show that yield pressures were reduced and the apparent tube compliance was increased by this intervention.

Because the mucus lining of an airway may have non-Newtonian properties, Hsu et al. (1994) used a similar experimental setup as Gaver et al. (1990), but with aqueous sodium alginate solutions with and without calcium chloride and sodium dodecyl sulfate. In various concentrations the resulting fluid ranged in surface tensions, storage and loss moduli, and shear viscosity. They found a similar dimensionless equation as Gaver et al. (1990), using the shear-dependent viscosity in their definition of *Ca*. However, at higher *Ca* they report a flow instability known as "stress-overshoot," which occurs when the time scale for deformation is shorter than the entanglement lifetime of these complex fluid macromolecules. Using non-Newtonian fluids described by power-law and Herschel-Buckley models with a solid-fluid shear yield stress, τ_y, similar experiments in a flattened, flexible tube (Low et al. 1997) find that increasing τ_y increases P_y.

4.2.2. THEORETICAL MODELS Gaver et al. (1996) developed a theoretical model of bubble propagation in a 2D flexible channel combining a lubrication approximation with a boundary-element method, where P_b drives the flow but also inflates the channel, whose liquid-filled portion far downstream has height $2H$. The theory exhibits two distinct types of behavior in its P_bH/σ-Ca relationship, denoted "pushing" and "peeling" (Figure 4). For low *Ca*, P_bH/σ decreases as *Ca* increases. In this "pushing" regime there is a long elastic transition region between the

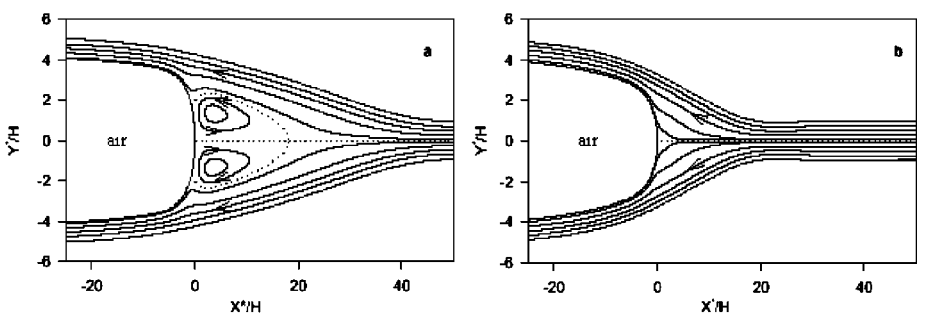

Figure 4 Steady-state streamlines for flow ahead of an air-finger forced through a liquid-filled, flexible channel with selected wall and fluid parameters. (*a*) Capillary number Ca = 0.2, recirculation region appears ahead of the air-finger (pushing mechanism). (*b*) Ca = 0.5, no recirculation region and the transition distance to the undisturbed, upstream channel height is shorter (peeling mechanism). From Gaver et al. (1996).

advancing meniscus in the upstream, wide part of the channel, and the first point where the channel height is $2H$. Increasing Ca causes a decrease in the elastic transition length. Consequently, the viscous resistance reduces and a lower $P_b H/\sigma$ is required to drive the flow. For large Ca the elastic transition distance is relatively short and the bubble tip is more pointed (Figure 4*b*). This is the peeling regime that is dominated by wall tension and fluid viscous forces, and for which $P_b H/\sigma$ increases with Ca (as seen experimentally). In this regime the channel wall has a sharp bend just ahead of the bubble tip: The low fluid pressure near the bend provides the adhesive force that must be overcome to reopen the channel. Adding surfactant to the system modifies the $P_b H/\sigma - Ca$ relationship. Yap & Gaver (1998) showed that the resulting Marangoni stresses generally require a larger driving pressure for any given Ca. Jensen et al. (2002) further investigated the peeling regime, showing that for large longitudinal tension the channel exhibits three distinct fluid-elastic regions: the wide inflated channel behind the bubble tip, the unopened channel ahead, and the bubble-tip region where the locally 2D flow acts like a low-Reynolds-number valve. Asymptotic solutions in these regions were formally matched together, giving an approximation of the $P_b H/\sigma - Ca$ relationship that compares well with numerical results. An extension of this model to account for unsteady effects captures the transient overshoot in P_b seen experimentally (Naire & Jensen 2003).

Heil (2000) investigated the propagation of a 2D bubble into a liquid-filled, flexible channel at finite Re. His numerical solution, using coupled finite-element discretizations of the free-surface Navier-Stokes equations and the Lagrangian wall equations, yields results at $Re = 0$ that compare well to those in Gaver et al. (1996). For $0 < Ca < 2$ and fixed values of the ratio Re/Ca ranging between 0 and 10, fluid inertia shifts the $P_b H/\sigma - Ca$ curve to higher pressures, approximately doubling the required pressure for $Re = 200$, $Ca = 2$. As Re increases in the peeling regime, low Bernoulli pressures influence the bend in the wall shape in the region ahead of the meniscus, and the bubble tip can become indented. Subsequently, this method was extended to describe the propagation of a 3D bubble into a nonaxisymmetric buckled tube at zero Re (Hazel & Heil 2003). Pushing and peeling solutions arise again: Remarkably, the 3D computations predict a $P_b H/\sigma - Ca$ relationship very similar to that identified using 2D models.

4.3. Liquid Plug Flows

Although the above models treat an advancing air finger, there are many instances where a liquid plug propagates in a flexible tube. Howell et al. (2000) modeled the quasi-steady propagation of a liquid plug through an elastic tube with a preexisting film, as one may find in airways. At low plug propagation speeds ($Ca \ll 1$), the analysis leads to a general form of the Landau-Levich equation modified for flexible walls that displace radially inward in the region of the plug. Asymptotic forms of the pressure drop across the plug and the ratio of the deposited film thickness to tube radius show a $Ca^{2/3}$-dependence. For weak longitudinal wall tension and small

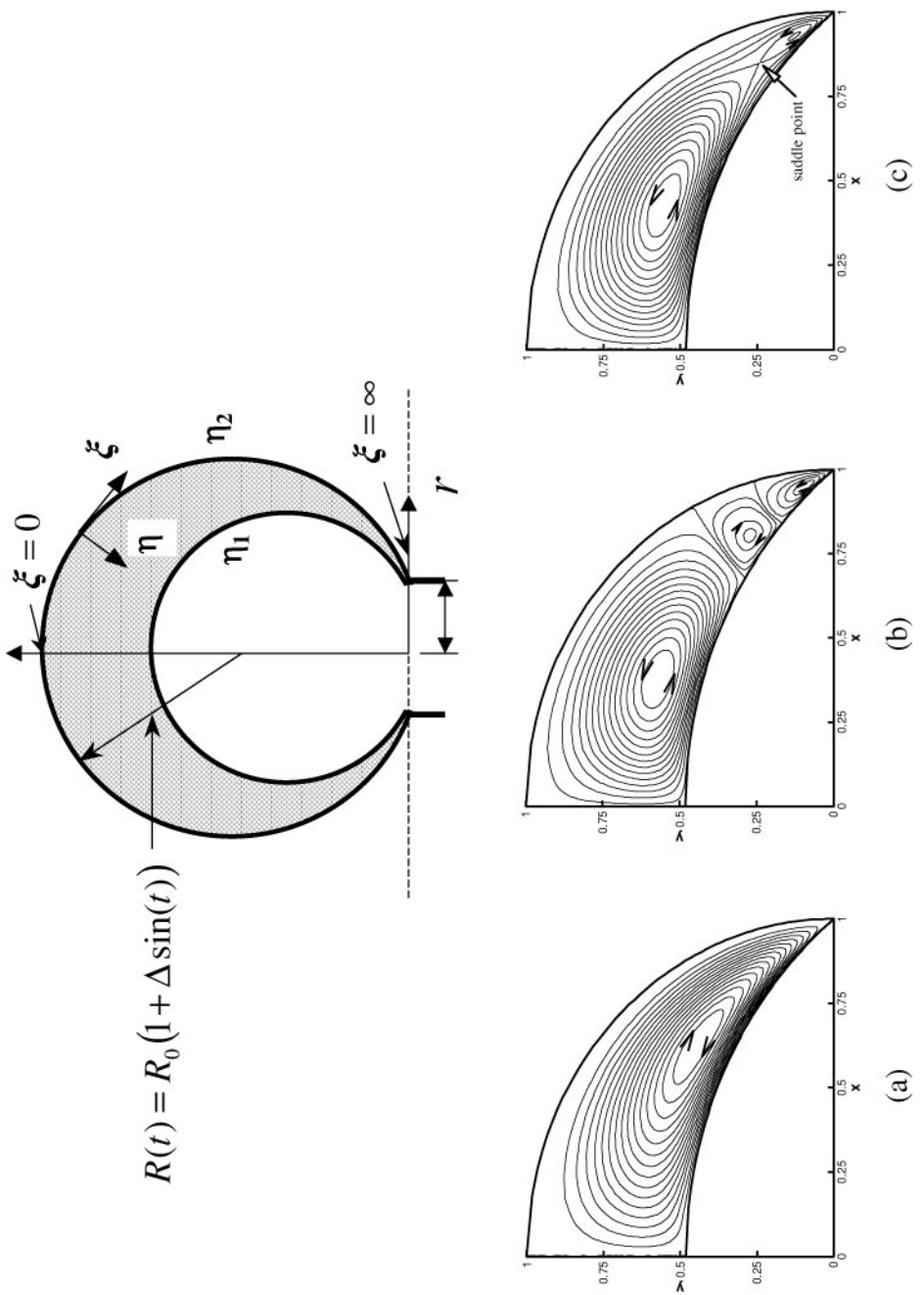
$R(t) = R_0(1 + \Delta \sin(t))$
$\xi = 0$
ξ
η
η_1
η_2
$\xi = \infty$
r
(a)
(b)
(c)
saddle point
x
y

wall compliance, both the wall displacement and the air-liquid interface curvature have the same $O(Ca^{1/3})$ axial boundary-layer thickness. For stronger wall tension, the wall boundary layer is significantly larger than the interfacial layer, requiring intermediate matching of these regions. The theory identifies the critical imposed pressure drop above which the bolus will eventually rupture because it deposits a thicker film than the precursor layer it picks up. The issues pertaining to liquid plug propagation and rupture are important for lung airway reopening phenomena.

4.4. Flow from Imposed Wall Stretch

Breathing motion of airway walls can move mucus. Espinosa & Kamm (1997) presented a mathematical model of a Newtonian fluid layer that starts with a uniform thickness and surfactant distribution as it rests on an extensible membrane. The membrane undergoes longitudinal cycling and the strain increases linearly along the wall so that there is a stiffer end (proximal airways) and a more flexible end (distal airways). Strain gradients induce surfactant concentration gradients that drive a Marangoni flow. Over the first imposed cycle they find that liquid transport toward the stiffer end (clearance) has an optimal frequency with maximal surface velocities in the range of 0.05 mm/sec, compared to 0.2 mm/sec produced by ciliary mechanisms. Increased strain amplitude diminishes transport and, in some cases, reverses the flow direction toward the distal end. Subsequently, Halpern et al. (submitted for publication) considered a cyclically stretching model of a branching airway network for surfactant transport into the lung, as may occur in surfactant replacement therapy. By fixing the film thickness and fluid pressure at both ends of the domain, and imposing a higher surfactant concentration at the proximal end, their model predicts that transport of surfactant into the lung is enhanced for larger strain amplitudes and frequency, though the latter is less important. The effect of frequency found in that model is opposite to the results in Bull & Grotberg (2003), where surfactant spreading over a thin liquid film coating a flexible sheet was studied. The film was contained within a cylindrical, flexible, vertical barrier (a well), and surfactant was introduced in the center region of the well. The sheet was stretched biaxially at different frequencies and the boundary conditions on the surfactant were no flux at the center and at the bounding well barrier. Under these conditions, increasing frequency reduces the overall Marangoni effect, and this is consistent with their accompanying theory.

←

Figure 5 Time-averaged streamlines of an oscillatory, alveolar flow described in bipolar coordinates. For fixed remaining parameters, the effect of surfactant is shown as a function of sorption parameter K: (*a*) $K = 0$ (insoluble surfactant), (*b*) $K = 0.8$, and (*c*) $K = 1.0$. The results are only drawn in a half domain of an alveolus due to the symmetry. For an insoluble surfactant as in (*a*), there is a clockwise, steady vortex. As K increases the structure can change to include three vortices (*b*), or even a saddle-point (*c*). From Wei et al. (2003).

At a smaller scale, the effect of imposed oscillations on alveolar liquid transport is important for local homeostasis. Podgorski & Gradon (1993) presented a flow model, based on earlier work (Gradon & Podgorski 1989), that is a liquid-lined, oscillating spherical cap whose opening is attached to an airway. An insoluble surfactant occupies the interface and the conditions at the opening are that surfactant and fluid may enter or leave the alveolus. The model predicts that fluid and surfactant will exit the alveolus due to a resulting Marangoni flow and, surprisingly, increasing fluid viscosity will increase the net outflow. Thus the alveolus is self-cleansing, though the cleansing is complete in this nonperiodic approach. A model that enables a periodic state, so that removed surfactant is replaced, is found in Zelig & Haber (2002). Their approach is to employ a source term in the surface transport equation for the insoluble surfactant. For alveoli that are surrounded by other alveoli, it can be more instructive to analyze a system where fluid outflow per cycle is negligibly small because there is no preferred direction, as occurs with the airway-attached alveolus. For thin liquid films in such a model, Wei et al. (2003) showed that time-averaged velocities provide a steady-streaming flow, which recirculates in the alveolus (Figure 5). The patterns can have multiple vortices whose size and direction depend on the system parameters. Thicker films enable more types of patterns, particularly as the inspiratory to expiratory time ratio changes.

5. OUTLOOK

Because of their complexity, the rich range of associated phenomena, and their biological relevance, studies of flow-structure interactions will remain at the heart of much of physiological fluid mechanics. Hopefully the problems described here illustrate the interest and the challenge of the field. Despite intensive investigation, the multiple mechanisms underlying the generation of instabilities in single-phase flow through flexible tubes (such as found in the Starling Resistor) remain incompletely understood. Present computational and asymptotic results give us only isolated glimpses of behavior in limited regions of parameter space, but emphasize the importance of global conditions. We must await more systematic investigations that will reveal generic relationships and phenomena relevant to experiments, which are necessarily 3D, and to physiological applications, for which the mechanical properties of tissues must be carefully accounted for. (Measurements of tissue deformability have not kept pace with the remarkable recent advances in imaging techniques allowing measurements of the geometry of an individual's blood vessels or airways.) Similarly, studies of topics such as airway closure and reopening have focused up to now on highly idealized model systems. While these have proved invaluable in identifying fundamental fluid-mechanical phenomena, there remains a considerable gulf between the predictions of these models and the likely behavior of real airways. New experiments giving insights into in vivo conditions, and new efforts to extend the capacity of existing models, are needed to bridge this divide.

The *Annual Review of Fluid Mechanics* is online at http://fluid.annualreviews.org

LITERATURE CITED

Bathe M, Kamm RD. 1999. A fluid-structure interaction finite element analysis of pulsatile blood flow through a compliant stenotic artery. *J. Biomech. Eng.-Trans. ASME* 121: 361–69

Bertram CD. 1986. Unstable equilibrium behavior in collapsible tubes. *J. Biomech.* 19:61–69

Bertram CD, Castles RJ. 1999. Flow limitation in uniform thick-walled collapsible tubes. *J. Fluids Struct.* 13:399–418

Bertram CD, de Tuesta GD, Nugent AH. 2001. Laser-Doppler measurements of velocities just downstream of a collapsible tube during flow-induced oscillations. *J. Biomech. Eng.-Trans. ASME* 123:493–99

Bertram CD, Godbole SA. 1997. LDA measurements of velocities in a simulated collapsed tube. *J. Biomech. Eng.-Trans. ASME* 119:357–63

Bertram CD, Raymond CJ, Butcher KSA. 1989. Oscillations in a collapsed-tube analog of the brachial artery under a sphygmomanometer cuff. *J. Biomech. Eng.* 111:185–91

Bertram CD, Raymond CJ, Pedley TJ. 1990. Mapping of instabilities for flow through collapsed tubes of differing length. *J. Fluids Struct.* 4:125–53

Bertram CD, Raymond CJ, Pedley TJ. 1991. Application of nonlinear dynamics concepts to the analysis of self-excited oscillations of a collapsible tube conveying a fluid. *J. Fluids Struct.* 5:391–426

Brook BS, Falle SAEG, Pedley TJ. 1999. Numerical solutions for unsteady gravity-driven flows in collapsible tubes: evolution and roll-wave instability of a steady state. *J. Fluid Mech.* 396:223–56

Brook BS, Pedley TJ. 2002. A model for time-dependent flow in (giraffe jugular) veins: uniform tube properties. *J. Biomech.* 35:95–107

Bull JL, Grotberg JB. 2003. Surfactant spreading on thin viscous films: film thickness evolution and periodic wall stretch. *Exp. Fluids* 34:1–15

Cancelli C, Pedley TJ. 1985. A separated-flow model for collapsible-tube oscillations. *J. Fluid Mech.* 157:375–404

Carew EO, Pedley TJ. 1997. An active membrane model for peristaltic pumping. 1. Periodic activation waves in an infinite tube. *J. Biomech. Eng.-Trans. ASME* 119:66–76

Carpenter PW, Berkouk K, Lucey AD. 1999. A theoretical model of pressure propagation in the human spinal CSF system. *Eng. Mech.* 6:213–28

Carpenter PW, Garrad AD. 1985. The hydrodynamic stability of flow over Kramer-type compliant surfaces. 1. Tollmien-Schlichting instabilities. *J. Fluid Mech.* 155:465–510

Carpenter PW, Garrad AD. 1986. The hydrodynamic stability of flow over Kramer-type compliant surfaces. 2. Flow-induced surface instabilities. *J. Fluid Mech.* 170:199–232

Carpenter PW, Pedley TJ. 2003. *Flow Past Highly Compliant Boundaries and in Collapsible Tubes*. Dordrecht, The Netherlands: Kluwer Academic

Dai GH, Gertler JP, Kamm RD. 1999. The effects of external compression on venous blood flow and tissue deformation in the lower leg. *J. Biomech. Eng.-Trans. ASME* 121:557–64

Danahy DT, Ronan JA. 1974. Cervical venous hum in patients on chronic hemodialysis. *N. Engl. J. Med.* 291:237–39

Davies C, Carpenter PW. 1997a. Instabilities in a plane channel flow between compliant walls. *J. Fluid Mech.* 352:205–43

Davies C, Carpenter PW. 1997b. Numerical simulation of the evolution of Tollmien-Schlichting waves over finite compliant panels. *J. Fluid Mech.* 335:361–92

de Vries MP, Schutte HK, Veldman AEP, Verkerke GJ. 2002. Glottal flow through a two-mass model: Comparison of Navier-Stokes

solutions with simplified models. *J. Acoust. Soc. Am.* 111:1847–53
Demiray H. 1996. Solitary waves in prestressed elastic tubes. *Bull. Math. Biol.* 58:939–55
Elad D, Kamm RD, Shapiro AH. 1987. Choking phenomena in a lung-like model. *J. Biomech. Eng.-Trans. ASME* 109:1–9
Espinosa FF, Kamm RD. 1997. Thin layer flows due to surface tension gradients over a membrane undergoing non-uniform, periodic strain. *Ann. Biomed. Eng.* 25:913–25
Everett DH, Haynes JM. 1972. Model studies of capillary condensation 1. Cylindrical pore model with zero contact angle. *J. Colloid Interface Sci.* 38:125–37
Eytan O, Elad D. 1999. Analysis of intra-uterine fluid motion induced by uterine contractions. *Bull. Math. Biol.* 61:221–38
Flaherty JE, Keller JB, Rubinow SI. 1972. Post-buckling behavior of elastic tubes and rings with opposite sides in contact. *SIAM J. Appl. Math.* 23:446–55
Gauglitz PA, Radke CJ. 1988. An extended evolution equation for liquid-film breakup in cylindrical capillaries. *Chem. Eng. Sci.* 43:1457–65
Gaver III DP, Halpern D, Jensen OE, Grotberg JB. 1996. The steady motion of a semi-infinite bubble through a flexible-walled channel. *J. Fluid Mech.* 319:25–65
Gaver III DP, Samsel RW, Solway J. 1990. Effects of surface tension and viscosity on airway reopening. *J. Appl. Physiol.* 69:74–85
Gavriely N, Shee TR, Cugell DW, Grotberg JB. 1989. Flutter in flow-limited collapsible tubes—a mechanism for generation of wheezes. *J. Appl. Physiol.* 66:2251–61
Ghadiali SN, Banks J, Swarts JD. 2002. Effect of surface tension and surfactant administration on Eustachian tube mechanics. *J. Appl. Physiol.* 93:1007–14
Gradon L, Podgorski A. 1989. Hydrodynamical model of pulmonary clearance. *Chem. Eng. Sci.* 44:741–49
Griffiths DJ. 1989. Flow of urine through the ureter: a collapsible, muscular tube undergoing peristalsis. *J. Biomech. Eng.-Trans. ASME* 111:206–11
Grotberg JB. 1994. Pulmonary flow and transport phenomena. *Annu. Rev. Fluid Mech.* 26:529–71
Grotberg JB. 2001. Respiratory fluid mechanics and transport processes. *Annu. Rev. Biomed. Eng.* 3:421–57
Guiot C, Pianta PG, Cancelli C, Pedley TJ. 1990. Prediction of coronary blood-flow with a numerical-model based on collapsible tube dynamics. *Am. J. Physiol.* 258:H1606–14
Guneratne JC. 1999. *High Reynolds number flow in a collapsible channel*. PhD thesis. Univ. Cambridge
Halpern D, Grotberg JB. 1992. Fluid-elastic instabilities of liquid-lined flexible tubes. *J. Fluid Mech.* 244:615–32
Halpern D, Grotberg JB. 1993. Surfactant effects on fluid-elastic instabilities of liquid-lined flexible tubes—a model of airway-closure. *J. Biomech. Eng.-Trans. ASME* 115:271–77
Halpern D, Grotberg JB. 2003. Nonlinear saturation of the Rayleigh instability in a liquid-lined tube due to oscillatory flow. *J. Fluid Mech.* In press
Hayashi S, Hayase T, Kawamura H. 1998. Numerical analysis for stability and self-excited oscillation in collapsible tube flow. *J. Biomech. Eng.-Tran. ASME* 120:468–75
Hazel AL, Heil M. 2003. Three-dimensional airway reopening: the steady propagation of a semi-infinite bubble into a buckled elastic tube. *J. Fluid Mech.* 478:47–70
Hazel AL, Heil M. 2003. Steady finite-Reynolds-number flows in three-dimensional collapsible tubes. *J. Fluid Mech.* 486:79–103
Heil M. 1997. Stokes flow in collapsible tubes: computation and experiment. *J. Fluid Mech.* 353:285–312
Heil M. 1999a. Airway closure: Occluding liquid bridges in strongly buckled elastic tubes. *J. Biomech. Eng.-Trans. ASME* 121:487–93
Heil M. 1999b. Minimal liquid bridges in non-axisymmetrically buckled elastic tubes. *J. Fluid Mech.* 380:309–37
Heil M. 2000. Finite Reynolds number effects in the propagation of an air finger into a

liquid-filled flexible-walled channel. *J. Fluid Mech.* 424:21–44

Heil M, Jensen OE. 2003. Flows in deformable tubes and channels: Theoretical models and biological applications. In *Flow Past Highly Compliant Boundaries and in Collapsible Tubes*, ed. PW Carpenter, TJ Pedley. Dordrecht, The Netherlands: Kluwer Academic

Heil M, Pedley TJ. 1996. Large post-buckling deformations of cylindrical shells conveying viscous flow. *J. Fluids Struct.* 10:565–99

Heil M, White JP. 2002. Airway closure: surface-tension-driven non-axisymmetric instabilities of liquid-lined elastic rings. *J. Fluid Mech.* 462:79–109

Hill MJ, Wilson TA, Lambert RK. 1997. Effects of surface tension and intraluminal fluid on mechanics of small airways. *J. Appl. Physiol.* 82:233–39

Howell PD, Waters SL, Grotberg JB. 2000. The propagation of a liquid bolus along a liquid-lined flexible tube. *J. Fluid Mech.* 406:309–35

Hsu SH, Strohl KP, Jamieson AM. 1994. Role of viscoelasticity in tube model of airway reopening. 1. Non-Newtonian sols. *J. Appl. Physiol.* 76:2481–89

Huang L. 1998. Reversal of the Bernoulli effect and channel flutter. *J. Fluids Struct.* 12:131–51

Huang L. 2001. Viscous flutter of a finite elastic membrane in Poiseuille flow. *J. Fluids Struct.* 15:1061–88

Ikeda T, Matsuzaki Y, Aomatsu T. 2001. A numerical analysis of phonation using a two-dimensional flexible channel model of the vocal folds. *J. Biomech. Eng.-Trans. ASME* 123:571–79

Ishizaka K, Flanagan JL. 1972. Synthesis of voiced sounds from a two-mass model of the vocal chords. *Bell Syst. Technol. J.* 51:1233–68

Jensen OE. 1990. Instabilities of flow in a collapsed tube. *J. Fluid Mech.* 220:623–59

Jensen OE. 1992. Chaotic oscillations in a simple collapsible-tube model. *J. Biomech. Eng.-Trans. ASME* 114:55–59

Jensen OE, Heil M. 2003. High-frequency self-excited oscillations in a collapsible-channel flow. *J. Fluid Mech.* 481:235–68

Jensen OE, Horsburgh MK, Halpern D, Gaver DP. 2002. The steady propagation of a bubble in a flexible-walled channel: Asymptotic and computational models. *Phys. Fluids.* 14:443–57

Kamm RD. 1987. Flow through collapsible tubes. In *Handbook of Bioengineering*, ed. S Chien. New York: McGraw-Hill

Kamm RD, Pedley TJ. 1989. Flow in collapsible tubes: a brief review. *J. Biomech. Eng.-Trans. ASME* 111:177–79

Kamm RD, Schroter RC. 1989. Is airway-closure caused by a liquid-film instability? *Respir. Physiol.* 75:141–56

Khir AW, O'Brien A, Gibbs JSR, Parker KH. 2001. Determination of wave speed and wave separation in arteries. *J. Biomech.* 34:1145–55

Knowlton FP, Starling EH. 1912. The influence of variations in temperature and blood-pressure on the performance of the isolated mammalian heart. *J. Physiol.-London* 44:206–19

Kounanis K, Mathioulakis DS. 1999. Experimental flow study within a self oscillating collapsible tube. *J. Fluids Struct.* 13:61–73

Kriegsmann JJ, Miksis MJ, Vanden-Broeck JM. 1998. Pressure driven disturbances on a thin viscous film. *Phys. Fluids.* 10:1249–55

Ku DN. 1997. Blood flow in arteries. *Annu. Rev. Fluid Mech.* 29:399–434

Kumaran V. 2000. Classification of instabilities in the flow past flexible surfaces. *Curr. Sci.* 79:766–73

Kumaran V. 2003. Hydrodynamic stability of flow through compliant channels and tubes. In *Flow Past Highly Compliant Boundaries and in Collapsible Tubes*, ed. PW Carpenter, TJ Pedley. Dordrecht, The Netherlands: Kluwer Academic

LaRose PG, Grotberg JB. 1997. Flutter and long-wave instabilities in compliant channels conveying developing flows. *J. Fluid Mech.* 331:37–58

Leuprecht A, Perktold K, Prosi M, Berk T, Trubel W, Schima H. 2002. Numerical study

of hemodynamics and wall mechanics in distal end-to-side anastomoses of bypass grafts. *J. Biomech.* 35:225–36

Li MJ, Brasseur JG. 1993. Nonsteady peristaltic transport in finite-length tubes. *J. Fluid Mech.* 248:129–51

Low HT, Chew YT, Zhou CW. 1997. Pulmonary airway reopening: effects of non-Newtonian fluid viscosity. *J. Biomech. Eng.* 119:298–308

Luo XY, Pedley TJ. 1995. A numerical-simulation of steady flow in a 2-D collapsible channel. *J. Fluids Struct.* 9:149–74

Luo XY, Pedley TJ. 1996. A numerical simulation of unsteady flow in a two-dimensional collapsible channel. *J. Fluid Mech.* 314:191–225

Luo XY, Pedley TJ. 1998. The effects of wall inertia on flow in a two-dimensional collapsible channel. *J. Fluid Mech.* 363:253–80

Luo XY, Pedley TJ. 2000. Multiple solutions and flow limitation in collapsible channel flows. *J. Fluid Mech.* 420:301–24

Matsuzaki Y, Ikeda T, Kitagawa T, Sakata S. 1994. Analysis of flow in a 2-dimensional collapsible channel using universal tube law. *J. Biomech. Eng.-Trans. ASME* 116:469–76

Miles JW. 1957. On the generation of surface waves by shear flows. *J. Fluid Mech.* 3:185–204

Naire S, Jensen OE. 2003. An asymptotic model of unsteady airway reopening. *J. Biomech. Eng.-Trans. ASME*. In press

Naureckas ET, Dawson CA, Gerber BS, Gaver III DP, Gerber HL, et al. 1994. Airway reopening pressure in isolated rat lungs. *J. Appl. Physiol.* 76:1372–77

Otis DR, Johnson M, Pedley TJ, Kamm RD. 1993. Role of pulmonary surfactant in airway-closure—a computational study. *J. Appl. Physiol.* 75:1323–33

Pal A, Brasseur JG. 2002. The mechanical advantage of local longitudinal shortening on peristaltic transport. *J. Biomech. Eng.-Trans. ASME* 124:94–100

Parker KH, Jones CJH. 1990. Forward and backward running waves in the arteries—analysis using the method of characteristics. *J. Biomech. Eng.-Trans. ASME* 112:322–26

Pedley TJ. 1980. *The fluid mechanics of large blood vessels*: Cambridge Univ. Press

Pedley TJ. 1992. Longitudinal tension variation in collapsible channels—a new mechanism for the breakdown of steady flow. *J. Biomech. Eng.-Trans. ASME* 114:60–67

Pedley TJ, Brook BS, Seymour RS. 1996. Blood pressure and flow rate in the giraffe jugular vein. *Philos. Trans. R. Soc. Lond. B. Biol. Sci.* 351:855–66

Pedley TJ, Luo XY. 1998. Modelling flow and oscillations in collapsible tubes. *Theor. Comput. Fluid Dyn.* 10:277–94

Pedley TJ, Stephanoff KD. 1985. Flow along a channel with a time-dependent indentation in one wall—the generation of vorticity waves. *J. Fluid Mech.* 160:337–67

Perktold K, Rappitsch G. 1995. Computer-simulation of local blood-flow and vessel mechanics in a compliant carotid-artery bifurcation model. *J. Biomech.* 28:845–56

Perun ML, Gaver III DP. 1995a. An experimental-model investigation of the opening of a collapsed untethered pulmonary airway. *J. Biomech. Eng.-Trans. ASME* 117:245–53

Perun ML, Gaver III DP. 1995b. Interaction between airway lining fluid forces and parenchymal tethering during pulmonary airway reopening. *J. Appl. Physiol.* 79:1717–28

Podgorski A, Gradon L. 1993. An improved mathematical model of hydrodynamic self-cleansing of pulmonary alveoli. *Ann. Occup. Hyg.* 37(4):347–65

Pozrikidis C. 2000. Instability of two annular layers or a liquid thread bounded by an elastic membrane. *J. Fluid Mech.* 405:211–41

Ralph ME, Pedley TJ. 1988. Flow in a channel with a moving indentation. *J. Fluid Mech.* 190:87–112

Rast MP. 1994. Simultaneous solution of the Navier-Stokes and elastic membrane equations by finite-element method. *Int. J. Numer. Methods Fluids.* 19:1115–35

Rosenzweig J, Jensen OE. 2002. Capillary-elastic instabilities of liquid-lined lung

airways. *J. Biomech. Eng.-Trans. ASME* 124: 650–55

Salacinski HJ, Goldner S, Giudiceandrea A, Hamilton G, Seifalian AM, et al. 2001. The mechanical behavior of vascular grafts: a review. *J. Biomater. Appl.* 15:241–78

Selverov KP, Stone HA. 2001. Peristaltically driven channel flows with applications toward micromixing. *Phys. Fluids.* 13:1837–59

Shankar V, Kumaran V. 1999. Stability of non-parabolic flow in a flexible tube. *J. Fluid Mech.* 395:211–36

Shapiro AH. 1977a. *Physiologic and medical aspects of flow in collapsible tubes*. Proc. 6th Can. Congr. Appl. Mech., Vancouver

Shapiro AH. 1977b. Steady flow in collapsible tubes. *J. Biomech. Eng.-Trans. ASME* 99:126–47

Shim EB, Kamm RD. 2002. Numerical simulation of steady flow in a compliant tube or channel with tapered wall thickness. *J. Fluids Struct.* 16:1009–27

Steinecke I, Herzel H. 1995. Bifurcations in an asymmetric vocal-fold model. *J. Acoust. Soc. Am.* 97:1874–84

Steinman DA, Ethier CR. 1994. The effect of wall distensibility on flow in a 2-dimensional end-to-side anastomosis. *J. Biomech. Eng.-Trans. ASME* 116:294–301

Story BH, Titze IR. 1995. Voice simulation with a body-cover model of the vocal folds. *J. Acoust. Soc. Am.* 97:1249–60

Tam ASM, Sapp MC, Roach MR. 1998. The effect of tear depth on the propagation of aortic dissections in isolated porcine thoracic aorta. *J. Biomech.* 31:673–76

Tang D, Yang J, Yang C, Ku DN. 1999. A nonlinear axisymmetric model with fluid-wall interactions for steady viscous flow in stenotic elastic tubes. *J. Biomech. Eng.-Trans. ASME* 121:494–501

Ur A, Gordon M. 1970. Origin of Korotkoff sounds. *Am. J. Physiol.* 218:524–29

Walsh C. 1995. Flutter in one-dimensional collapsible tubes. *J. Fluids Struct.* 9:393–408

Wang DM, Tarbell JM. 1992. Nonlinear-analysis of flow in an elastic tube (artery)-steady streaming effects. *J. Fluid Mech.* 239:341–58

Wang DM, Tarbell JM. 1995. Nonlinear-analysis of oscillatory flow, with a nonzero mean, in an elastic tube (artery). *J. Biomech. Eng.-Trans. ASME* 117:127–35

Wei HH, Benintendi SW, Halpern D, Grotberg JB. 2003. Cycle-induced flow and transport in a model alveolar liquid lining. *J. Fluid Mech.* 483:1–36

Yap DYK, Gaver III DP. 1998. The influence of surfactant on two-phase flow in a flexible-walled channel under bulk equilibrium conditions. *Phys. Fluids.* 10:1846–63

Yi MQ, Bau HH, Hu H. 2002. Peristaltically induced motion in a closed cavity with two vibrating walls. *Phys. Fluids.* 14:184–97

Zelig D, Haber S. 2002. Hydrodynamic cleansing of pulmonary alveoli. *SIAM J. Appl. Math.* 63:195–221

Zhao W, Zhang C, Frankel SH, Mongeau L. 2002. Computational aeroacoustics of phonation, Part I: Computational methods and sound generation mechanisms. *J. Acoust. Soc. Am.* 112:2134–46